PAPER • OPEN ACCESS

Flat Proton Spectra in Large Solar Energetic Particle Events

View the article online for updates and enhancements.

IOP ebooks™

Bringing you innovative digital publishing with leading voices to create your essential collection of books in STEM research.

Start exploring the collection - download the first chapter of every title for free.

Flat Proton Spectra in Large Solar Energetic Particle Events

D Lario[1], L Berger[2], L B Wilson III[3], R B Decker[1], D K Haggerty[1], E C Roelof[1], R F Wimmer-Schweingruber[2] and J Giacalone[4]

[1]The Johns Hopkins University. Applied Physics Laboratory
[2]Institut für Experimentelle und Angewandte Physik (IEAP). Christian-Albrechts-Universität zu Kiel
[3]NASA, Goddard Space Flight Center
[4]Lunar and Planetary Laboratory. University of Arizona

Corresponding author's e-mail: david.lario@jhuapl.edu

Abstract. We present solar energetic particle events observed at 1 AU from the Sun for which the proton energy spectra at energies between ~50 keV to ~1 MeV flatten during a period of at least ~12 hours prior to the passage of the associated interplanetary shock. The flattening of the proton energy spectra occurs when the source of the particles (presumably the traveling interplanetary shock) is still downwind from the spacecraft and particle intensities are still continuously increasing. The arrival of the shock at the spacecraft is then characterized by a steepening of the spectra, where low-energy proton intensities show a more pronounced enhancement than the high-energy proton intensities. We discuss the mechanisms that may result in this flattening of the spectra in terms of current models presented in the literature.

1. Introduction

The time evolution of the solar energetic particle (SEP) intensities measured in interplanetary (IP) space depends on both the acceleration processes responsible for the energization of the particles and the transport processes undergone by the particles during their travel from their sources to the observing spacecraft. Both the acceleration and the transport processes depend on a large number of factors, among them the energy achieved by the particle, which controls its ability to escape from the acceleration region and regulates the effects that the ambient medium has on its transport before reaching a spacecraft. The evolution of the kinetic energy spectra of the particles measured at a given heliospheric location during a SEP event provides information of the acceleration mechanisms undergone by the particles once the processes of particle transport and particle release from their acceleration region have been properly deconvolved.

Several functional forms have been adopted to describe the particle energy spectra integrated over the duration of a SEP event [e.g., 1, 2]. However, in order to determine the time history of the acceleration processes, an analysis of the precise temporal evolution of the energy spectra throughout the SEP event is required. This type of analysis shows how the energy spectra evolve from the onset of the event, when the most energetic particles arrive at the spacecraft, to later times when the energy spectra typically straighten into a power-law shape at low energies mostly in association with the arrival of IP shocks [e.g., 3, 4, 5]. Related to the processes of particle acceleration at IP shocks, the study of the energy spectra around the passage of shocks has revealed a broad range of energy spectra and diverse time evolutions that depend, among other factors, on the properties of the shocks [e.g., 6, 7, 8, 9]. However, the shock parameters alone do not unequivocally determine the characteristics of the energetic particle enhancements observed in association with the passage of the shocks [10].

Here we pay attention to a recurrently observed peculiarity in intense SEP events associated with the passage of IP shocks. Long time intervals of at least ~12 hours are observed before the passage of the shocks showing flat proton energy spectra (in the energy range between ~50 keV and ~1 MeV) that only steepen when the shock approaches the spacecraft when low-energy proton intensities become more abundant than higher-energy intensities. We corroborate that those periods are commonly observed by a diversity of energetic particle instruments on board spacecraft located at ~1 AU from the Sun. Therefore, unless all particle instruments have similar functional problems, this phenomenon results from an actual physical mechanism that culminates in the measurement of equal proton intensities at different energies. Since those periods occur when the traveling shock is still far from the spacecraft, we believe that the mechanism responsible for their observation is predominantly related to the processes of particle escape from the vicinity of the shock and their subsequent transport to the spacecraft, rather than the shock acceleration process itself.

2. Observations

The Low-Energy Magnetic Spectrometer (LEMS120) telescope of the Electron Proton and Alpha Monitor (EPAM) on the Advanced Composition Explorer (ACE) measures ions between ~47 keV and 4.8 MeV in eight differential energy channels [11]. The magnet or open (O) semi-conductor detector telescope (SST-O) of the Three-Dimensional Plasma and Energetic Particle Investigation (3DP) on board the Wind spacecraft measures ions from a few tens of keV up to 11 MeV [12, 13]. Neither ACE/EPAM/LEMS120 nor Wind/3DP/SST distinguish among protons, alpha particles and other ion species. We will assume that intensities measured by both instruments are dominated by protons and the contribution of alpha particles and heavy ions is small compared to that of protons. The Energetic Particle Sensor (EPS) on board the Geostationary Operational Environmental Satellites (GOES) detects protons in eight energy intervals ranging from 0.8-4.2 MeV up to 200-500 MeV in the case of GOES-11 [14, 15]. The combination of the Low Energy Detector (LED) and High Energy Detector (HED) of the Energetic and Relativistic Nuclei and Electron (ERNE) experiment on board the Solar and Heliospheric Observatory (SOHO) provides proton intensities in the energy range from ~1 MeV to hundreds of MeV [16]. This assortment of energetic particle instruments allows us to build continuous proton energy spectra covering a broad range of energies starting just above ~50 keV.

Figure 1 shows four intense SEP events where long-time intervals with flat energy spectra were observed. Each panel shows, from top to bottom, (i) proton intensities measured by (a-b) ACE/EPAM/LEMS120 and GOES-11/EPS and (c-d) ACE/EPAM/LEMS120 and SOHO/ERNE; (ii) the proton solar wind speed measured by the Solar Wind Electron Proton Alpha Monitor (SWEPAM) on board ACE [17]; and (iii) the magnetic field magnitude as observed by the Magnetic Field Experiment on board ACE [18] (when gaps of ACE/SWEPAM data exist we overplot, using red dots, proton solar wind speed data from the Solar Wind Experiment (SWE) on board the Wind spacecraft [19] shifted to the time of the shock passage at ACE). Table 1 summarizes the main properties of the solar flares and plane-of-sky CME speeds associated with the origin of the SEP events included in this study as well as the arrival times of the associated IP shocks. The black vertical arrows in Figure 1 indicate the time of the parent solar flares and the solid vertical lines the passage of IP shocks by the ACE spacecraft. The dashed vertical lines in panels (a) and (c) indicate the passage of the leading edge of the interplanetary counterpart of coronal mass ejections (ICMEs) as identified by Richardson and Cane [20].

The tilted gray rectangles in Figure 1 indicate the time intervals when flat low-energy proton spectra were observed. These periods are easily identifiable as those time-intervals when intensities at different energies overlap. We have indicated in panels (b) and (d) with dotted traces those periods when the low-energy channels of ACE/EPAM/LEMS120 showed contamination due to high-energy particles penetrating in the instrument that occurs mainly at the onset of the SEP events. In these two events (Figures 1b and 1d), the flat energy spectra period was observed when the contribution of these high-energy particles in the respective channels had already diminished.

For the events in panels (a) and (b), the flat spectra were observed over the energy range from ~68

keV up to ~2-3 MeV starting several hours before the arrival of the shocks. Considering the average transit speed of the shock to travel from the Sun to 1 AU (last column in Table 1), at the time when these flat spectra started being observed, the shocks were located at ~0.5 and ~0.6 AU from the spacecraft for the events (a) and (b), respectively. Whereas in panel (a) flat spectra were observed almost up to the shock arrival, in panel (b) the intensities at different energies separated out as the shock approached the spacecraft resulting in steeper energy spectra at the time of the shock passage.

For the event in panel (c), the flat-spectra period started ~17 hours before the shock passage, i.e. when the shock was still ~0.4 AU away from spacecraft (assuming that it propagated at the averaged transit speed quoted in Table 1). The flat spectra continued until the shock arrival even when low-energy intensities were still increasing. The energy range over which these flat spectra were observed extended from ~50 keV up to ~0.5 MeV.

For the event in panel (d), the flat spectra developed about ~17 hours after the onset of the event when low-energy particles gradually began to arrive at the spacecraft. However, the low-energy intensities started to separate about ~17 hours before the shock arrival (when the shock was ~0.3 AU away from the spacecraft considering that the shock propagated at the average transit speed quoted in Table 1).
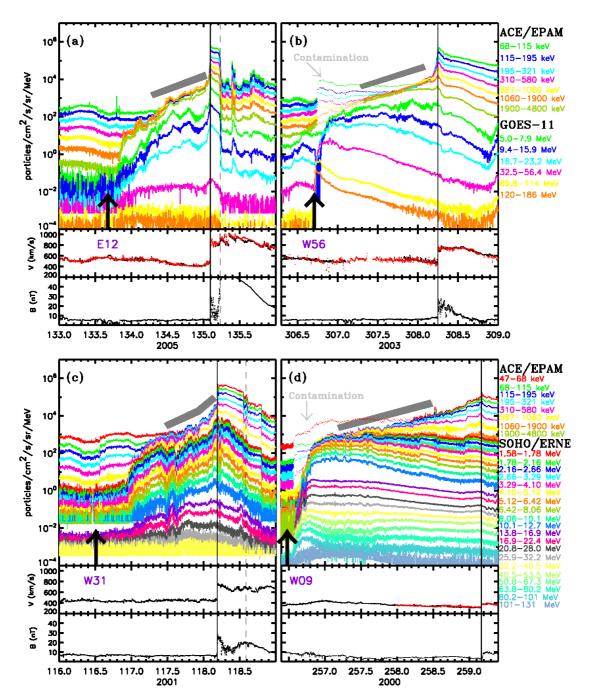
One may wonder whether the observation of these flat-spectra periods is due to an instrumental effect. Figure 2 shows the same set of events shown in Figure 1 but using Wind/3DP/SST-O data. The time-intensity profiles, the intensities at the different energy channels, and the periods with flat-spectra were similar as those observed by ACE/EPAM/LEMS120. Either, both instruments had a similar malfunction or the development of the flat-spectra periods responds to a real physical mechanism.

Table 1. Main properties of the solar flares and shocks associated with the selected SEP events
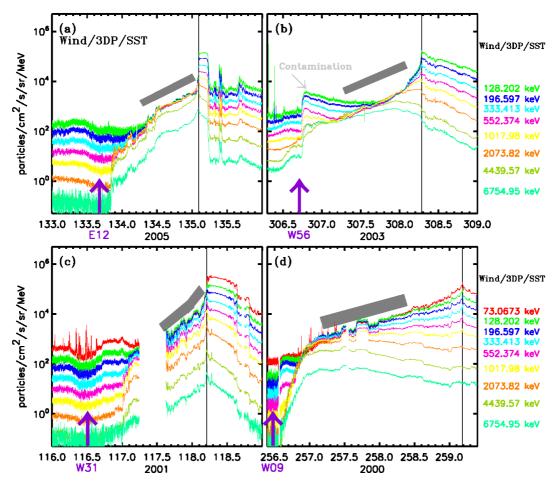
Event	Flare SXR onset time yy/doy/hh:mm	Flare Class	Flare Site	CME (km/s)[a]	Shock time passage doy/hh:mm	Average shock transit speed (km/s)
Figs. 1(a)-2(a)	05/133/16:13	M8.0/2B	N12E12	1689	135/02:11	1223
Figs. 1(b)-2(b)	03/306/17:03	X8.3/2B	S14W56	2598	308/05:59	1125
Figs. 1(c)-2(c)	01/116/12:11	M7.8/2B	N17W31	1006	118/04:31	1030
Figs. 1(d)-2(d)	00/256/11:31	M1.0/2N	S17W09	1550	259/03:59	645
Fig. 3(a)	00/313/22:42	M7.4/1N	N10W77	1738	315/06:19	1314
Fig. 3(b)	78/266/09:47	/2B	N35W50	-	268/07:18*	913
Fig. 3(c)	98/273/13:08	M2.8/2N	N23W81	-	275/06:53	995
Fig. 3(d)	74/262/22:53	/2B	N08W63	-	264/12:45*	1097
Fig. 4(a)	12/147/~20:35	-	N16W122	1966	149/02:48	1375
Fig. 4(b)	11/080/02:15	-	N16W130	1341	081/18:05	1043
Fig. 5	12/067/00:02	X5.4/3B	N17E27	2684	068/10:45	1197
	12/067/01:05	X1.3/SF	N22E12	1825		

[a] CME plane-of-sky speed as reported in the catalog of CMEs observed by SOHO at cdaw.gsfc.nasa.gov/CME_list/

*Time of a Sudden Storm Commencement used as a proxy for the time of IP shock passage
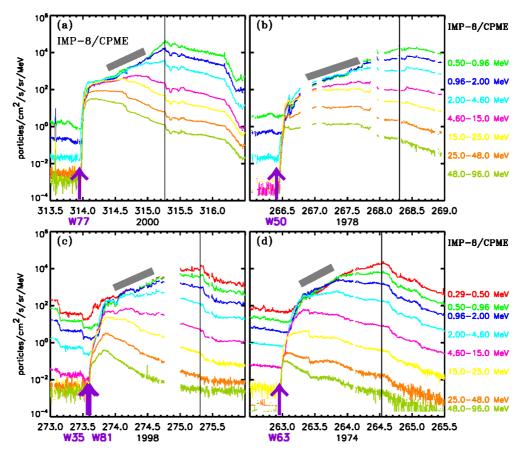
Figure 1. One-minute averages of the spin-averaged ion intensities measured by ACE/EPAM/LEMS120 and of the proton intensities measured by GOES-11-EPS (panels a and b) and by SOHO/ERNE (panels c and d), together with the proton solar wind speed measured by ACE/SWEPAM and the magnetic field magnitude measured by the magnetic field experiment on board ACE. The black arrows indicate the occurrence of the solar eruption that generated the event at the longitude indicated below. The vertical solid lines indicate the passage of IP shocks, and the dashed vertical lines the leading edge of ICMEs. The tilted gray rectangles indicate the periods when flat spectra at low energies (<~1 MeV) were observed. The noisy 47-68 keV ion channel from ACE/EPAM/LEMS120 during the events in panels (a) and (b) has not been represented. The red dots in the solar wind panels indicate Wind/SWE data shifted to the time of the shock at ACE.

Figure 2. Wind/3DP/SST-O spin-averaged ion intensities for the same events shown in Figure 1.

We have also performed a search for SEP events showing flat-spectra periods in historical data records. The Charged Particle Measurement Experiment (CPME) on board the Interplanetary Monitoring Platform (IMP-8) measured protons in ten differential channels over the energy range 0.29-145 MeV [21]. The stack of detectors and the on-board logic allowed a distinction between proton, alpha, and Z≥3 heavy ions. Alpha particle intensities were used to correct some of the proton channels that were also sensitive to alpha particles [21]. Figure 3 shows some of the SEP events selected within the IMP-8/CPME data set for which long-lasting flat-spectra periods were observed. The properties of the parent solar flares for these SEP events are listed in Table 1. The IMP-8 SEP events showing periods with flat spectra were also associated with the passage of IP shocks (in the column of Table 1 with the times of the shock passage, we have indicated with an asterisk those times when a Sudden Storm Commencement was used as a proxy for an IP shock passage instead of an actual shock observed in magnetic field and solar wind plasma data). Since IMP-8/CPME data do not reach the low proton energies measured by ACE/EPAM/LEMS120 and Wind/3DP/SST-O, the effects of the shock passage on the intensity-time profiles are not so accentuated as for the events shown in Figures 1 and 2. The flat spectra in the events in Figures 3(a) and 3(b) extended up to ~4.6 MeV, whereas for the events in Figures 3(c) and 3(d) they extended up to ~2 MeV, with intensities still increasing. Several hours before the shock arrival, proton intensities at different energies separated resulting in energy spectra that steepened.

Figure 3. 5.5-minute averages of proton intensities measured by IMP-8/CPME in four selected events. The solid vertical lines indicate the passage of the interplanetary shocks and the purple arrows the occurrence of the parent solar eruption as described in Table 1. Note that for the event in panel (c) two solar eruptions may be responsible for the SEP event and the IP shock as described in [22].
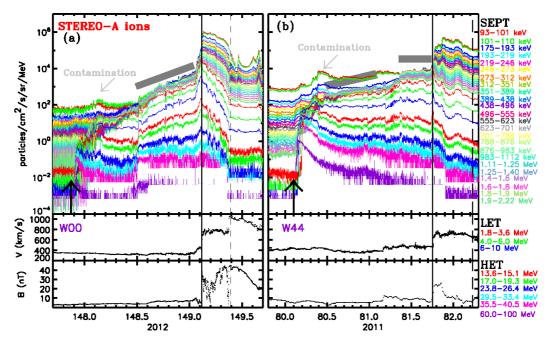
More recent data sets also show some SEP events with flat-spectra periods. Figure 4 shows two SEP events observed by the suite of energetic particle instruments of the In-situ Measurements of Particles And CME Transients (IMPACT) on board the spacecraft A of the Solar TErrestrial RElations Observatory (STEREO-A) [23]. IMPACT consists of a series of telescopes; in particular, the Solar Electron and Proton Telescope (SEPT) that measures ions from ~60 to 6500 keV in 32 energy bins without distinguishing protons from alpha particles or other heavy ions [24], the Low-Energy Telescope (LET) that measures protons from 1.8 to ~15 MeV [25] and the High-Energy Telescope (HET) that measures protons from 13 to ~100 MeV [26]. It is important to mention that, similarly to ACE/EPAM/LEMS120 and Wind/3DP/SST-O, STEREO/SEPT ion channels might have some contamination by electrons and high-energy particles penetrating into the ion telescope apertures, especially at the onset of intense SEP events (as indicated in Figure 4). Moreover, during periods of reduced counts rates at low energies (such as in a flat-spectra period) but with significant ion fluxes above 2.2 MeV, limitations in the SEPT electronics produce extra counts in specific low-energy bins. These bins have not been included in Figure 4. Such caveats in the STEREO/SEPT data are described in detail in [27].

Figure 4 shows that, after the periods with possible contamination in the low-energy channels early in the events, flat-spectra developed prior to the arrival of the shocks. For the event in Figure 4(a), the flat energy spectra extended up to ~2 MeV with intensities still increasing. For the event in Figure 4(b), a first period with flat-spectra starting on day ~80.5 and extending up to ~2 MeV was observed, when the lower energy channels were still contaminated by penetrating high-energy particles. Just

prior to the arrival of the shock in Figure 4(b), another flat-spectra interval was observed extending up to ~1 MeV with almost flat intensity-time profiles.

Figure 4. One-minute averages of, from top to bottom, ion intensities averaged over the four telescopes of STEREO-A/SEPT and proton intensities as measured by STEREO-A/LET and STEREO-A/HET, solar wind proton speed and magnetic field as measured by the Plasma and Suprathermal Ion Composition (PLASTIC) investigation [28] and the Magnetic Field Experiment on board STEREO-A [29]. The black arrows indicate the occurrence of the solar eruption that generated the event at the indicated longitude (longitude given with respect to STEREO-A, see [30]). The vertical solid lines indicate the passage of IP shocks, and the dashed vertical lines the leading edge of ICMEs. The gray tilted rectangles indicate the time intervals where the energy spectra at low energies flatten.

3. Discussion

The examples shown in the previous section illustrate some of the SEP events where long-lasting periods (>12 h) with flat proton energy spectra (mostly at energies below 1 or 2 MeV) are observed. These SEP events tend to be intense and associated with the passage of interplanetary shocks. The flat-spectra periods are usually observed prior to the arrival of the shocks when low-energy proton intensities are still increasing. The arrival of the shock is usually characterized by a subsequent intensity increase, where low-energy proton intensities show a more pronounced enhancement than the high-energy proton intensities, resulting in a steepening of the energy spectra.

The continuous injection and acceleration of particles by the approaching traveling IP shock seems to be a common characteristic of these events. Hybrid simulations of particle acceleration at shocks, including processes produced by magnetic field fluctuations excited by the shock-accelerated particles propagating in the upstream region of the shocks, predict similar intensities of protons at different energies at a certain distance upstream of the shock [e.g., 31]. At small upstream distances from the shock, the lower the energy of the particles the more intense the event becomes, resulting in a softer energy spectrum (see Figure 1e in [31]). Whereas these simulations are consistent with the observations, the limited simulation domain of these models does not allow us to analyze how far from the shock and up to what energies these flat spectra can extend.

As a matter of fact, the events analyzed in Section 2 show that the observation of these flat-spectra

periods starts when the shocks are still located at large distances downwind from the spacecraft and continues for a long-lasting interval. It is well-known that the observation of shock-accelerated particles by spacecraft located at 1 AU depends not only on the processes of particle acceleration at the approaching shock, but also on the particle release from the vicinity of the shock and the subsequent particle transport from the shock up to the spacecraft. Particle acceleration may start as soon as the shock forms close to the corona [32] and continues as the shock expands into the IP medium and passes the spacecraft at 1 AU [33]. The conditions of particle acceleration at the shock throughout all this time may vary, not only because shock properties change as the shock propagates but also because the spacecraft establishes magnetic connection with different regions of the shock where shock parameters and particle acceleration conditions vary as the shock expands toward the spacecraft [34]. Therefore, the flattening of these spectra intervals must be more a consequence of the processes of particle escape from the shock vicinity and particle transport toward the spacecraft rather than the varying processes of particle acceleration at the shock.

Several models have been developed over the years to couple the propagation of IP shocks as a mobile source of shock-accelerated particles and the transport of SEPs in IP space [e.g., 35-41, and references therein]. Some of these models have been developed in earlier efforts that modeled simultaneous observations of SEP events by multiple spacecraft (i.e. Helios, ISEE-3 and IMP-8) [e.g., 42, 34]. In particular, the models by Li et al. [38] and Hu et al. [39] included particle acceleration processes via the diffusive shock acceleration mechanism in a series of shells formed around the shock. These models predict hard energy spectra early in the SEP events as observed at 1 AU from the Sun that with time extend to low energies (as slower particles reach the spacecraft) and soften as the shock approaches 1 AU and becomes less and less efficient at accelerating particles to higher energies (cf., Figures 8-11 in [38] and Figures 9-10 in [39]). These models consider that, once particles escape from the shock vicinity where they are accelerated, their propagation in the upstream unperturbed solar wind is described by a focused-diffusion transport where the strength of the pitch-angle scattering processes is taken from a 2D-slab turbulence model conveniently scaled with radial distance and particle energy. The predicted energy spectrum integrated over time-intervals of different durations shows that early in the SEP events it may flatten with energy but quickly steepens after a few hours (e.g., ~6 hours after the shock initiation time in Figures 9-10 in [39]). The evolution of the energy spectra in such models depends on the combination of the particle acceleration processes at the region magnetically connected with the observer, the escape of particles from the shock complex, and the processes of particle transport in IP space.

The flat-spectra periods shown in Section 2 are instantaneously observed (as opposite to integrated over time) and start not just after the onset of the SEP event but when the shocks are already located at some distance from the Sun (for example, at ~0.3-0.6 AU from the Sun for the events in Figures 1 and 2). That the flat-spectra periods are observed in intense SEP events (all of them associated with fast CMEs, see Table 1), are of long duration (>12 h), and occur while particle intensities are still increasing, suggest that the intensity of the event and the way particles propagate from a strong shock able to inject a large number of particles toward the spacecraft play essential roles in the development of these flat spectra.
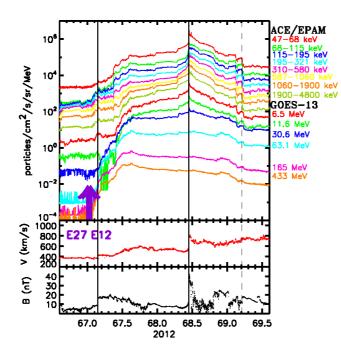
The model of Ng et al. [41] coupled the evolution of the shock accelerated particles with that of Alfvén waves in the solar wind (where the wave growth depended on the momentum gradients of the particle populations and shock acceleration was represented by a continuous injection of particles with a prescribed temporal evolution and energy source spectra). This model predicts proton energy spectra that flatten at some energy below ~10 MeV and that can be observed only after a certain time has passed since the onset of the SEP event (e.g., Figures 6 and 9 in [41]). In this model, high-energy protons streaming outward from the shock amplify the pre-existing ambient Alfvén waves, in such a way that the slower low-energy protons, as well as energetic minor ions, find themselves traveling through resonant Alfvén waves previously amplified by the higher velocity protons. The process results in a self-regulatory mechanism where the waves amplified by the higher-energy protons control the transport of the lower-energy protons. The harder the spectra of the injected shock-accelerated

particles the faster the growth of the amplified waves, and hence the stronger the effect on the lower energy particle transport. The result is a retardation of the outward SEP transport by the moving region of amplified waves, generating regions of flat intensity spatial profiles behind this region but steep profiles in and ahead of this region. The measurement of a flat-energy spectrum by a distant spacecraft depends on how this region of amplified waves propagates, how the particle acceleration at the shock evolves, and how the waves are continuously amplified by the higher energy protons. The model, however, predicts flat-spectra intervals of short duration (e.g., Figure 8 in [41]) that contrast with the long-lasting periods shown in Section 2.

Le Roux and Webb [43] developed a time-dependent focused transport model to investigate particle acceleration at fast IP shocks via first-order Fermi mechanism with a prescribed Alfvén wave spectrum upstream and across the shock to scatter the particles. A minimum particle speed is required for the particles traveling along the magnetic field to stay ahead of the traveling shock, which depends on the shock speed V_{sh}, the angle between the upstream magnetic field and the shock normal θ_{Bn}, and the particle speed along the magnetic field $v\mu$ (where μ is the particle pitch-angle and v is the particle speed). Whereas particles with $v\mu < (V_{sh}-V_{sw})sec(\theta_{Bn})$ cannot escape from the shock vicinity and participate in the acceleration processes, particles with $v\mu > (V_{sh}-V_{sw})sec(\theta_{Bn})$ are capable of moving forward along the magnetic field (where V_{sw} is the upstream solar wind speed). The result is that the energy spectra observed at some distance from the shock show (i) a deficit of particles at the energies corresponding to the shock speed, (ii) a flattening at higher energies corresponding to particle speeds and pitch-angles μ such that their escape from the shock vicinity is impeded, and (iii) a decrease at even higher intensities (e.g., Figure 3a in [43]). The arrival of the shock is then characterized by a steepening of the energy spectra coinciding with the arrival of the particles confined in the shock vicinity. Note that the temporal evolution of V_{sh} and θ_{Bn}, as well as the varying conditions for particle scattering close to the shock during the transit of the shock from the Sun to 1 AU lead to different conditions for particle escape from the shock vicinity. Therefore, this mechanism needs to include this variability to be consistent with the long-lasting flat spectra observed in multiple events.

According to these models, both the capability of the particles to escape from the shock vicinity and the interactions undergone by the particles during their transport to the spacecraft are at the root of the observation of these flat-spectra periods. The amplification of waves by high-energy particles seems to play an essential role in the transport of the lower energy particles [41]. Most of the SEP events exhibiting flat-energy spectra shown in Section 2 are intense and associated with solar eruptions capable of generating >100 MeV protons. However, for the SEP events shown in Figures 1(c) and 4(a), the contribution of high-energy particles was minimal. In most cases, the flat-spectra periods were observed when the high-energy intensities had already declined suggesting that, if they were the cause of the amplification of the resonating Alfvén waves, those were generated earlier in the event and did not decay throughout the event. We note that the presence of these amplified waves did not limit the intensities measured at 1 AU, since in most of the cases particle intensities continued to increase even when flat energy spectra were observed.

The elevated intensities and the presence of high-energy protons do not seem to be conditions necessary for the observation of flat-spectra at low energies. For example, Figure 5 shows an intense SEP event measured by ACE/EPAM/LEMS120 and GOES-13 with elevated intensities (even higher than those of the events shown in Section 2) and where even ~400 MeV protons were observed. The origin of the shock in this event may be related to two consecutive solar eruptions [44], and the elevated proton intensities might have resulted from the passage of a pre-existing IP shock early on day 67 [45]. It is possible that the pre-conditioning of the ambient medium may inhibit the amplification of Alfvén waves [46] and hence prevent the formation of SEP flat spectra. Therefore, the medium where the particles propagate plays also a role in the observation of flat-spectra intervals.

Figure 5. Five-minute averages of spin-averaged ion intensities measured by ACE/EPAM/LEMS120 and of proton intensities as measured by GOES-13-SEM during an intense SEP event in March 2012, together with the proton solar wind speed as measured by Wind/SWE and the magnetic field magnitude as measured by the magnetic field experiment on board ACE. The purple arrows indicate the occurrence of the solar eruptions that generated the event at the longitude indicated below. The vertical solid lines indicate the passage of interplanetary shocks, and the dashed vertical line the leading edge of an ICME.

4. Conclusions

The goal of this paper is to highlight the peculiarity of long-lasting periods with flat energy spectra observed in intense SEP events associated with the passage of IP shocks, especially at low-energies, from about ~50 keV up to about ~1 MeV. The processes by which shock-accelerated particles propagate from the shock toward the observer are likely the dominant causes for the formation of these flat-spectra periods, where the amplification of Alfvén waves supposedly plays a substantial role. A straightforward question to ask concerns the extension of these spectra to energies below the lower thresholds of the energetic particle instruments, i.e. whether these spectra continue flat to energies below ~50 keV, or their intensities rise with decreasing energy up to the more abundant thermal particle intensities. Extended measurements of proton distributions from solar wind thermal through suprathermal energies for this type of events will be analyzed in future works.

References

[1] Mewaldt R A, Looper M D, Cohen C M S, Haggerty D K, Labrador A W, Leske R A, Mason G M, Mazur J E and von Rosenvinge T T 2012 *Space Sci. Rev.* **171** 97
[2] Desai M I, Mason G M, Dayeh M A, Ebert R W, McComas D J, Li G, Cohen C M S, Mewaldt R A, Schwadron N A and Smith C W 2016 *Astrophys. J.* **816** 68
[3] Doran D J and Dalla S 2016 *Solar Phys.* **291** 2071
[4] Laurenza M, Consolini G, Storini M and Damiani A 2012 *Astrophys. Space Sci. Trans.* **8** 19
[5] Laurenza M, Consolini G, Storini M and Damiani A 2015 *J. Phys. Conf. Ser.* **632** 012066
[6] van Nes P, Reinhard R, Sanderson T, Wenzel K-P and Zwickl R 1984 *J. Geophys. Res.* **89** 2122
[7] Ho G C, Lario D, Decker R B, Smith C W and Hu Q 2008 *AIP Conf. Proc.* **1039** 184
[8] Laurenza M, Consolini G, Storini M, Pallocchia G and Damiani A 2016 *J. Phys. Conf. Ser.* **767**

012015

[9]   Pallocchia G, Laurenza M, Consolini G 2017 *Astrophys. J.* **837** 158

[10]   Lario D, Hu Q, Ho G C, Decker R B, Roelof E C and Smith C W 2005 Proc. Solar Wind 11/ SOHO 16, Connecting Sun and Heliosphere (Eds. B Fleck et al.), ESA SP **592** 81

[11]   Gold R E, Krimigis S M, Hawkins S E, Haggerty D K, Lohr D A, Fiore E, Armstrong T P, Holland G and Lanzerotti L J 1998 *Space. Sci. Rev.* **86** 541

[12]   Lin R P, Anderson K A, Ashford S, Carlson C et al. 1995 *Space. Sci. Rev.* **71** 125

[13]   Wilson III L B, Cattell C A, Kellog P J, Goetz K et al. 2010 *J. Geophys. Res.* **115** A12104

[14]   Onsager T G, Grubb R, Kunches J, Matheson L, Speich D, Zwickl R and Sauer H 1996 *Proc. SPIE (Ed. E R Washwell)* **2812** 281

[15]   Sandberg I, Jiggens P, Heynderickx and Daglis I A 2014 *Geophys. Res. Lett.* **41** 4435

[16]   Torsti J, Valtonen E, Lumme M, Peltonen P, Eronen T, et al. 1995 *Solar Phys.* **162** 505

[17]   McComas D J, Bame S J, Baker P, Feldman W C, Phillips J L, Riley P and Griffee J W 1998 *Space. Sci. Rev.* **86** 563

[18]   Smith C W, L'Heureux J, Ness N F, Acuna M H, Burlaga L et al. 1998 *Space. Sci. Rev.* **86** 613

[19]   Ogilvie K W, Chornay D J, Fritzenreiter R J, Hunsaker F., et al. 1995 *Space. Sci. Rev.* **71** 55

[20]   Richardson I G and Cane H V 2017 www.srl.caltech.edu/ACE/ASC/DATA/level3/icmetable2

[21]   Sarris E T, Krimigis S M and Armstrong T P 1976 *J. Geophys. Res.* **81** 2341

[22]   Lario D, Marsden R G, Sanderson T R, Maksimovic M et al. 2000 *J. Geophys. Res.* **105** 18251

[23]   Luhmann J G, Curtis D W, Scroeder P, et al. 2008 *Space. Sci. Rev.* **136** 117

[24]   Muller-Mellin R, Bottcher S, Falenski J, Rode E, et al. 2008 *Space. Sci. Rev.* **136** 363

[25]   Mewaldt R A, Cohen C M S, Cook W R, Cummings A C et al. 2008 *Space. Sci. Rev.* **136** 285

[26]   von Rosenvinge T T, Reames D V, Baker R, Hawk J, et al. 2008 *Space. Sci. Rev.* **136** 391

[27]   Gomez-Herrero R 2013 "STEREO/SEPT Level 2 Science Data Format Specifications and Caveats" in www2.physik.uni-kiel.de/stereo/data/sept/level2/SEPT_L2_description.pdf

[28]   Galvin A B, Kistler L M, Popecki M A, Farrugia C J et al. 2008 *Space. Sci. Rev.* **136** 437

[29]   Acuna M H, Curtis D, Scheifele J L, Russell C T, Schroeder P, Szabo A and Luhmann J G 2008 *Space. Sci. Rev.* **136** 203

[30]   Lario D, Aran A, Gomez-Herrero R, Dresing N, Heber B, Ho G C, Decker R B and Roelof E C 2013 *Astrophys. J.* **767** 41

[31]   Giacalone J 2004 *Astrophys. J.* **609** 452

[32]   Lario D, Kwon R Y, Riley P and Raouafi N E 2017 *Astrophys. J.* **847** 103

[33]   Cane H V, Reames D V and von Rosenvinge T T 1988 *J. Geophys. Res.* **93** 95558

[34]   Lario D, Sanahuja B and Heras A M 1998 *Astrophys. J.* **509** 415

[35]   Pomoell J, Aran A, Jacobs C, Rodriguez-Gasen R, Poedts S and Sanahuja B 2015 *J. Space Weather and Space Climate* **5** A12, 10.1051/swsc/2015015

[36]   Luhmann J G, Mays M L, Odstrcil D, Li Y, Bain H, Lee C O, Galvin A B, Mewaldt R A, Cohen C M S, Leske R A, Larson D and Futaana Y 2017 *Space Weather* **15** 934

[37]   Schwadron N, Gorby M, Torok T, Downs C, et al. 2014 *Space Weather* **12** 323

[38]   Li G, Zank G P and Rice W K M 2003 *J. Geophys. Res.* **108** 1082, 10.1029/2002JA009666

[39]   Hu J, Li G, Ao X, Zank G P and Verkhoglyadova O 2017 *J. Geophys. Res.* **122** 10938

[40]   Boronikov D, Sokolov I V, Roussev I I, Taktakishvili A and Gombosi T I 2018, 2018arxiv180607030B

[41]   Ng C K, Reames D V and Tylka A J 2003 *Astrophys. J.* **591** 461

[42]   Heras A M, Sanahuja B, Lario D, Smith Z, Detman T and Dryer M 1995 *Astrophys. J.* **445** 497

[43]   Le Roux J A and Webb G 2012 *Astrophys. J.* **746** 104

[44]   Lario D, Ho G C, Roelof E C, Anderson B J and Korth H 2013 *J. Geophys. Res.* **118** 63

[45]   Lario D and Karelitz A 2014 *J. Geophys. Res.* **119** 4185

[46]   Lario D, Aran A and Decker R B 2008 *Space Weather* **6** S12001, 10.1029/2008SW000403